STRATEGIC GEOGRAPHIC POSITIONING OF SEA LEVEL GAUGES TO AID IN EARLY DETECTION OF TSUNAMIS IN THE INTRA-AMERICAS SEA

Joshua I. Henson[1], Frank Muller-Karger[1], Doug Wilson[2]
Steven L. Morey[3], George A. Maul[4], Mark Luther[1], Christine Kranenburg[1]

[1] College of Marine Science
University of South Florida
140 7th Ave S. St. Petersburg, FL 33705 United States

[2] Office of Atmospheric Research
National Oceanic and Atmospheric Administration
NOAA Chesapeake Bay Office Annapolis, MD 21403 United States

[3] Center for Ocean-Atmospheric Prediction Studies
Florida State University
Tallahassee, FL 32306 United States

[4] Department of Marine and Environmental Systems
Florida Institute of Technology
150 W. University Blvd Melbourne, FL 32901 United States

ABSTRACT

The potential impact of past Caribbean tsunamis generated by earthquakes and/or massive submarine slides/slumps, as well as the tsunamigenic potential and population distribution within the Intra-Americas Sea (IAS) is examined to help define the optimal location for coastal sea level gauges intended to serve as elements of a regional tsunami warning system. The goal of this study is to identify the minimum number of sea level gauge locations to aid in tsunami detection and provide the most warning time to the largest number of people. We identified 12 initial, prioritized locations for coastal sea level gauge installation. Our study area approximately encompasses 7ºN, 59ºW to 36ºN, 98ºW. The results of this systematic approach to assess priority locations for coastal sea level gauges will assist in developing a tsunami warning system (TWS) for the IAS by the National Oceanic and Atmospheric Administration (NOAA) and the Regional Sub-Commission for the Caribbean and Adjacent Regions (IOCARIBE-GOOS).

INTRODUCTION

Historical data suggest that tsunamis have occurred in the Intra-Americas Sea (IAS) region approximately once every 3-yr, and destructively once every 21-yr [*O'Loughlin and Lander*, 2003]. According to Bryant [2005], approximately 14% of all tsunamis have occurred in the Caribbean. When considering only Hawaii, Alaska, the U.S. West Coast, and the Caribbean, about 2,590 victims or 83% of all tsunami fatalities in these regions over the last 150 years occurred in the Caribbean [*O'Loughlin and Lander*, 2003]. As a result of these recorded fatalities and the rise of Caribbean population by almost 300% from 1950 to 2000 [*CIAT, et al.*, 2005], protection of human life is a primary reason for establishing a TWS in this region. In this work, historical tsunamis in the IAS are analyzed with the aid of a numerical ocean model and the results are used to suggest locations for coastal sea level gauges for the most efficient implementation of a TWS for the IAS region.

A tsunami is a series of large amplitude, shallow water gravity waves generated by an event capable of displacing a huge volume of water. Whether a gravity wave is considered to be a shallow or deep-water wave depends on the ratio between its wavelength and the depth of water.

Deep-water wave: $\lambda < 2\,H$
Shallow-water wave: $\lambda > 20\,H$

where, λ = wavelength and H = water depth

While tsunamis are usually generated in deep water, they are considered shallow-water waves because the typical wavelength of a tsunami is 220,000-m and the average depth of the Caribbean is approximately 2600-m.

Tsunamis propagate at the shallow water gravity wave phase speed of $c = (g\,H)^{1/2}$, which can be in excess of 222 m s^{-1} ($\sim$ 800 km hr^{-1}), until they dissipate or encounter a shelf and shallow coastal water where they slow to $8 - 14$ m s^{-1} ($\sim 30 - 50$ km hr^{-1}) [*NOAA and USGS Fact Sheet*, 2005]. Tsunami dissipation primarily depends on the magnitude and character of the tsunamigenic event, although bottom topography and bottom type also play important roles. Eventually, the tsunami is likely to impact a shoreline where life and property are then endangered. This study seeks to understand how and where tsunamis are generated in the IAS, how they travel through this region, and where a minimum number of sensors should be located to most efficiently warn the public of an impending tsunami.

A comprehensive warning system typically uses a seismometer to detect a geological event capable of generating a tsunami, and then utilizes near-by sea level gauges to determine whether a tsunami was generated. The system also should be able to predict potential impact locations and wave height, and disseminate that information to decision-makers. Different types of tsunami warning systems/networks are currently being successfully employed to measure, record, and telemeter both oceanographic and meteorological data. Standard means of telemetry include satellite, radio, cellular, telephone line, or Internet. One type of tsunami monitoring system involves Real-Time Kinematic Global Positioning System (RTK-GPS) technology [*Kato, et al.*, 2001]. Curtis [2001] suggests a multi-sensor approach. The Pacific TWS utilizes a combination of coastal sea level gauges and Deep-ocean Assessment and Reporting of Tsunamis (DART) buoys to acquire data for tsunami detection and for propagation and coastal run-up prediction.

The predominant tsunamigenic events are earthquakes; however landslides, avalanches, submarine slumps or slides, volcanic eruptions, volcano flank failure, and oceanic meteor impact can also cause a tsunami [*Lander, et al.*, 2002; *McCann*, 2006; *Pararas-Carayannis*, 2004]. Often, a tsunami is the result of coinciding events, thus it can be difficult to identify the actual tsunamigenic mechanism(s). Seismic and/or volcanic activity can produce a submarine landslide, which can in turn generate a tsunami. When analyzing events from pre-instrument periods it can be difficult to determine if a submarine slump or slide occurred, and the actual direct tsunamigenic event, such as this, may remain undetected. The manner in which a tsunami is generated will affect the warning time available [*Lander, et al.*, 1999]. This warning time can be maximized by predicting how and where the next IAS tsunami is most likely to occur. In general, the closer a sea level gauge is to a tsunami origin, the more warning time available to other locations around the Caribbean basin.

When designing a TWS it is critical to understand the types of tsunamigenic mechanisms, the coastlines that are more likely to be affected by a tsunami, tsunami travel time to those coasts, and the resulting effects from historical tsunamis [*Lander, et al.*, 1999]. However, the historical record is incomplete. In this study, we simulate tsunamigenic events with the potential to have far-field (greater than 1000-km) destructive impacts. The results of the numerical simulations are combined with information on human population concentrations around the Caribbean to determine the most critical and advantageous locations for the installation of coastal sea level gauges.

Discussed later, most sub-aerial landslides and volcanic tsunami origins are only locally destructive and are therefore not considered in this study. In order to determine if a tsunami is truly destructive at a location, high resolution bottom topography and a model with run-up capability is required to predict the extent of inundation. Wave height along the coast is not analyzed in this study because local effects dictate the necessity of very high bathymetric and model grid resolution to determine wave amplitude at the seashore. Run-up results along a coastline can vary by a factor of 10 [*Hwang and Lin*, 1969; *Smith and Shepherd*, 1994].

Historical Tsunamis in the IAS Region

Shallow earthquakes, magnitude 6.5 or greater, cause the majority of Caribbean tsunamis [*McCann*, 2006]. O'Loughlin and Lander [2003] describe 127 reported tsunamis in the Caribbean basin over approximately the past 500-yr. Of those reported, the authors find that 53 are almost certainly true tsunamis and another 8 are most likely true. These tsunami events were generated by various sources including but not limited to earthquakes, submarine slides/slumps, volcanic eruptions, and more likely a combination of those three. Understanding how past tsunamis have affected the region will help determine how future tsunami disasters can be mitigated.

The historical record of tsunami origins and affected areas is sparse. The data used in this study is from both O'Loughlin and Lander [2003] and the National Geophysical Data Center [*NGDC*, 2005]. These original tsunami origin data have 0.1° precision [*Dunbar*, 2005, personal correspondence], and while there are historical records of areas affected by some of these events, for others there is no information regarding effects or arrival location. Therefore, a numerical model is used to simulate historical tsunamis. Criteria used to select the events that are simulated are discussed under Methods ("Creation of Tsunamigenic Events List"). The simulations are performed with the Navy Coastal Ocean Model (NCOM), described under Methods ("Modeling").

The Caribbean and Surrounding Tectonic Plates

In order to fully understand the nature of the earthquakes that may generate tsunamis, the plate boundaries and their movement must also be understood. Tectonic activity due to plate movement is the principal cause of earthquakes, 80% of which occur along the plate boundaries in the oceanic crust [*Woods Hole*, 2005]. Figure 1 shows the plates in the Caribbean region, their boundaries, and summarizes their interactions. The Caribbean (CA) plate is bordered to the north and east by the North American (NA) and South American (SA) plates, to the south by the SA, North Andes (ND), Panama (PM), and Cocos (CO) plates, and to the west by the CO plate [*Bird*, 2003; *Lander, et al.*, 2002; *McCann*, 2006; *O'Loughlin and Lander*, 2003; *Pararas-Carayannis*, 2004]. Sitting on the CA plate are the islands of Hispaniola, Puerto Rico, and Jamaica to the north, the Lesser Antilles to the east, and to the west is Central America. The South American continent boarders the CA plate to the south [*Bird*, 2003; *McCann*, 2006].

The CA plate is moving eastward approximately 20 ± 3 mm yr^{-1} relative to the NA and SA plates [*Demets*, 1993; *Grindlay, et al.*, 2005; *Lander, et al.*, 2002; *McCann*, 2006; *O'Loughlin and Lander*, 2003; *Pararas-Carayannis*, 2004; *ten Brink, et al.*, 2004]. Some estimates are as high as 37 mm yr^{-1} [*Mercado and McCann*, 1998; *Sykes, et al.*, 1982]. The NA and SA plates are subducting under the eastern margin of the CA plate, leading to the formation of the Lesser Antilles volcanic arc. At the northern boundaries, the CA plate is sliding past the NA plate leading to transpressional motion (compressive loading as a result of shear stresses) and uneven or oblique subduction near Puerto Rico [*Lander, et al.*, 2002; *McCann*, 2006; *O'Loughlin and Lander*, 2003]. The southern boundary is characterized by a complex convergent margin near Venezuela and strike-slip faults on land [*McCann*, 2006]. The CO plate is subducting under the CA plate on the western boundary, which also forms a chain of volcanic activity [*Lander, et al.*, 2002]. Further explanation on the tectonic regime of the CA and adjacent plates can be found in McCann [2006] and Grindlay et al. [2005].
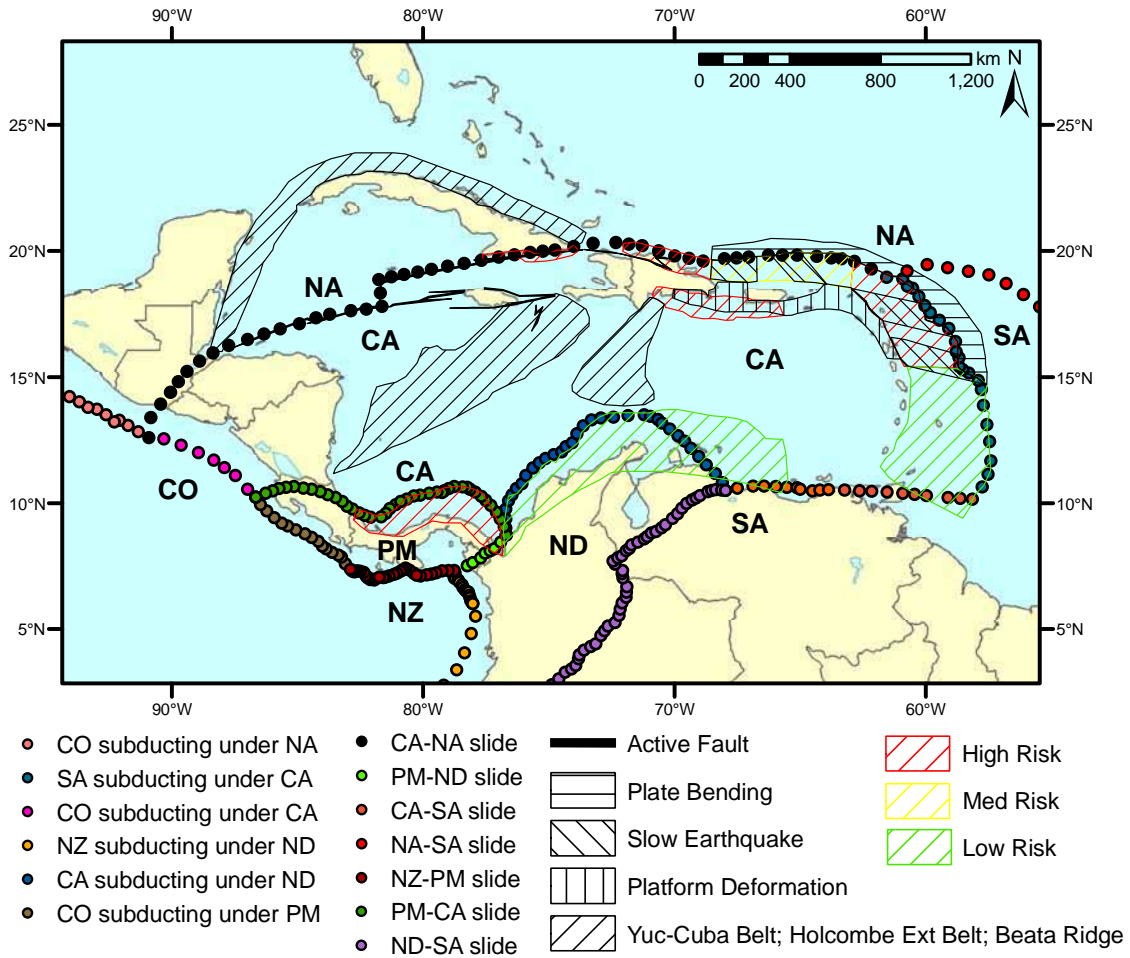
Figure 1 – Plate boundaries and interactions from Bird [2003] and tsunamigenic source regions from McCann [2006].

Tsunamigenic Earthquakes

There is a range of possible outcomes due to seismic activity in the Caribbean, some of which are more likely to produce a tsunami [*Grindlay, et al.*, 2005; *McCann*, 2006; *Mercado and McCann*, 1998]. The nature in which a tsunamigenic earthquake occurs will dictate the attributes of a resulting tsunami. Typically, significant vertical deformation of the sea floor (i.e. a dip/slip earthquake) is required for tsunami generation. This deformation can be due to either isostatic rebound of an accretionary prism near a subduction zone or a change in crustal elevation [*McCann*, 2006; *Okal, et al.*, 2003]. The direction of movement, depth of deformation, length and width of the deforming fault or plate boundary, deformation dip and slip angles, and focal depth will determine the size of the tsunami [*McCann*, 2006; *Polet and Kanamori*, 2000; *Zahibo, et al.*, 2003a]. For example, a shallow subduction zone earthquake or an earthquake with a more vertical angle of deformation will usually displace a larger volume of water and consequently generate a larger tsunami [*Bilek and Lay*, 2002; *Polet and Kanamori*, 2000]. The overlying geology also determines whether a tsunami will result from an earthquake [*Bilek and Lay*, 2002; *Kanamori*, 1972]. There may be stronger motion at the sea floor than the measured seismic moment would

typically represent if a rupture occurs within a sedimentary wedge or the rupture velocity is slow [*Okal, et al.*, 2003; *Polet and Kanamori*, 2000].

Regions where there is potential for an earthquake with a slow rupture velocity, or slow earthquake, to occur have a higher potential to produce a tsunami larger than a seismometer would otherwise indicate [*Polet and Kanamori*, 2000; *Todorovska and Trifunac*, 2001]. When the sea floor deformation velocity is on the same order as tsunami velocity (i.e. a slow earthquake, slide, or slump) the tsunami may be amplified by an order of magnitude [*Todorovska and Trifunac*, 2001]. The amplification may be caused by constructive interference as the tsunami is produced, since a slow rupture velocity will yield a longer duration earthquake [*Bilek and Lay*, 2002].

McCann [2006] defines seismic tsunamigenic threats in the Caribbean (see Figure 1) into the following categories: platform deformation, plate bending, slow earthquake, belts and ridges, active faults, and low to high tsunamigenic risk. These regions are based on the geologic and tectonic regime of the IAS, and the plate boundaries/interactions from Bird [2003] coincide with McCann's [2006] tsunamigenic zones.

Tsunamigenic Submarine Slides, Slumps and Landslides

These types of tsunamigenic events are typically initiated by an earthquake, hurricane, or volcanic event such as an eruption or flank failure, but they may also be initiated without an apparent catalyst [*Jiang and LeBlond*, 1992; *Lander, et al.*, 1999; *McCann*, 2006; *O'Loughlin and Lander*, 2003; *Pararas-Carayannis*, 2004; *von Huene, et al.*, 1989; *Grilli and Watts*, 2005]. Therefore, it may be difficult to determine whether a slide or an earthquake is the source of a tsunami. For example, the tsunami can be caused by a slide or slump that may or may not be related to an earthquake.

Many tsunamis have been generated in areas of the Caribbean where strike/slip plate movements dominate tectonic activity [*McCann*, 2006]. This suggests a slide or slump as either the primary or secondary tsunamigenic mechanism because vertical deformation of the sea floor is not typically associated with strike/slip plate movement. Grindlay et al. [2005] shows historic evidence of massive slumps or slides along the northern Puerto Rico margin which most likely generated tsunamis, and cracking on the eastern edge of the Mona rift that may lead to mass failures in the future, similar to past events.

Understanding how a tsunami forms helps determine their propagation and destructive potential. Since slide or slump tsunami-like waves have a much shorter period than a more typical dip/slip type tsunami, they dissipate faster and are typically only locally dangerous [*Fryer and Watts*, 2000; *Fryer, et al.*, 2001; *Pararas-Carayannis*, 2004; *Watts, et al.*, 2003]. Without detailed ocean bottom mapping and analysis it is difficult to determine the potential for a massive slide or slump. Hence, the slide or slump tsunamigenic potential of the IAS is not considered in this work.

Tsunamigenic Volcanic Events

Volcanoes along the Lesser Antilles chain are the most likely source for volcanic tsunamigenic events in the Caribbean Sea. Overall, approximately 5% of tsunamis are volcanic in origin [*O'Loughlin and Lander*, 2003; *Sigurdsson*, 1996]. There are many different volcanic tsunamigenic mechanisms from eruption to structural failure. O'Loughlin and Lander [2003] and Pararas-Carayannis [2004] review case studies of such events, including tsunamis that were generated by the Soufrière Hills volcano on Montserrat Island, the Mt. Pelèe volcano on

Martinique, the La Soufrière volcano on St. Vincent, and Kick'em Jenny, a submarine volcano north of Grenada affecting Montserrat, Martinique, St. Vincent, and Grenada, respectively.

Most tsunamis of volcanic origin have relatively local destructive effects and/or are predictable. This limits how useful a basin wide TWS will be to protect the public from volcanic tsunamigenic events. Therefore, these events are not considered in this study. The best defense against local tsunamis is public education.

Sea Level Gauges in the Caribbean and Adjacent Regions

Over approximately the past 10-yr, some 60 sea level gauge stations were installed in the Caribbean and surrounding countries by NOAA, programs such as RONMAC (Water Level Observation Network for Latin America) and CPACC (Caribbean Planning for Adaptation to Global Climate Change), and other locally and internationally-funded programs to examine local sea level changes and other weather related research. Government organizations, educational institutions, and independent companies had offered to maintain these stations, but as of February 2006, most stations are in various states of disrepair. The majority of which no longer collect data, and in many cases, installations are missing equipment. To contribute to a tsunami warning network, most stations will need to be replaced, while others need to be upgraded with additional hardware such as a Global Positioning System (GPS) receiver and/or Geostationary Operations Environmental Satellite (GOES) transmitter [*Henson and Wilson*, 2005].

As of February 2006, of the 60 stations that had been deployed historically throughout the IAS region, 17 are fully operational and transmitting data, 16 are not operational but the equipment was accounted for, and 10 are questionably operational. The remaining stations are either no longer operational or missing altogether [*Air-Sea Monitoring Systems*, 2006; *Henson and Wilson*, 2005]. Groups such as IOCARIBE, the Puerto Rico Seismic Network (PRSN), and NOAA are working towards the installation of sea level gauges throughout the IAS (see Results and Discussion "Operational Sea Level Gauges in the Caribbean").

METHODS

This study seeks to determine where the minimum number of sea level gauges should be located to maximize the warning time to the largest amount of people. We analyze how and where regionally destructive tsunamis form, propagate, and impact a coastline, as well as the coastal population distribution. We also develop an assessment of where coastal sea level gauges are operational so monitoring efforts will not be duplicated.

Without pinpointing specific tsunami origin locations, we examine areas where a tsunami is more likely to occur by using a tsunamigenic event source map [*McCann*, 2006] and the known or assumed origins of 42 historical tsunamis. This analysis is critical to maximizing warning time because a sea level gauge should be installed closest to a tsunami origin. Propagation, travel time, and impact analyses are accomplished through the simulation of historical tsunamis with the NCOM. There are several sub-studies involved in using the NCOM including parameter sensitivity and initial condition analyses, and travel time calculations [*Henson*, 2006]. The amount of warning time available is derived from a combination of modeling with the NCOM, developing isochrones, and estimating travel time to coastal population centers throughout the region. Isochrones were developed independently and then tested against the NCOM results.

The tsunamigenic risk analysis uses a 1° resolution grid whereas the NCOM uses a 2-arc-minute resolution grid. The former is used to determine where a tsunami is most likely to occur, and the latter is used to understand tsunami propagation and travel time.

Creation of Tsunamigenic Events List

A total of 61 tsunamis have affected the IAS region in the past 500-yr. Event data is taken from both O'Loughlin and Lander [2003] and the NGDC tsunami database [2005]. Since most volcanic and shore-based landslide tsunamigenic events have localized effects, they are omitted from this study [*O'Loughlin and Lander*, 2003; *Pararas-Carayannis*, 2004; *Smith and Shepherd*, 1995]. Events are also discarded if the origin is located inland, the origin latitude and longitude cannot be found, or the event did not originate in the IAS.

Each event is qualitatively rated on a scale of 0 – 4 according to the validity of the historical observations, and we chose the higher of the ratings from the two databases of rankings available [*NGDC*, 2005; *O'Loughlin and Lander*, 2003]. In an effort to create the largest list of probable events, the 42 simulated historical events have a validity rating of 3 or higher. All simulated tsunamigenic sources are assumed to be regionally destructive.

It is necessary to adjust some of the historical origin coordinates to properly initialize the NCOM (due to model bottom topography and grid resolution limitations). Where possible, the origin is moved closer to or along a plate boundary, but in some cases they are moved perpendicular to isobaths. Figure 2 shows the final origin locations of the simulated tsunamis. Table 1 provides a list of the events modeled and notes which origins were adjusted.
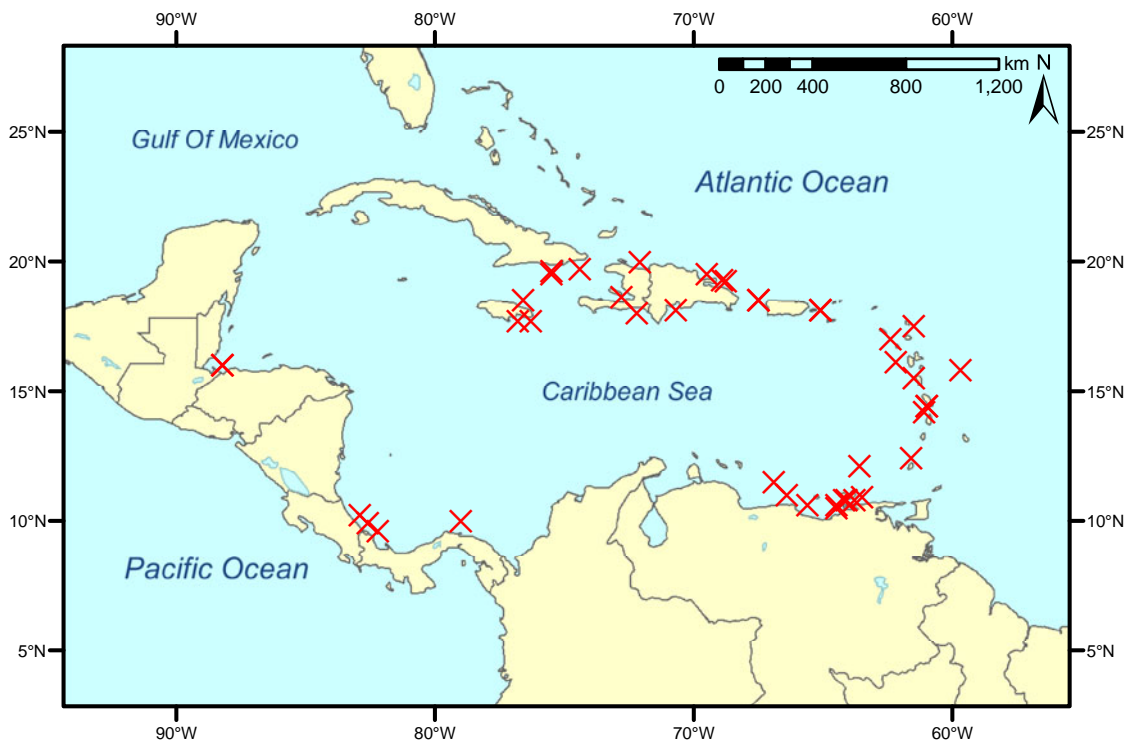

Figure 2 – The locations of the 42 historical tsunamis simulated in this study. The origin of the tsunamigenic events are represented by an "X" (see Table 1). Some events have a similar origin location.

Table 1 – Tsunami events modeled, ordered chronologically (see also Figure 2). Shaded cells denote events whose origin is adjusted, with original coordinates shown in parenthesis. Sources: O'Loughlin and Lander [2003] and the NGDC Tsunami Database [2005]. No information was found for cells that are blank.

Tsunami origin	Latitude (°N)	Longitude (°W)	Date	Time	Validity rating	Earthquake magnitude and corresponding scale	Source type and brief description
Venezuela	10.80 (10.70)	64.20 (64.20)	9/1/1530	1430 UT	4		Earthquake
S. Belize	16.00 (16.20)	88.20 (88.50)	11/24/1539	2300 LT	4		Earthquake
Venezuela	10.80 (10.70)	64.10 (64.10)	9/1/1543	2300 LT	4		Earthquake
Leeward Is.	17.50	61.50	4/16/1690		4	Ms 8.0	Earthquake; dispute regarding exact day, found 4/06/1690 as well
Jamaica	17.70 (17.90)	76.80 (76.90)	6/7/1692	1643 UT	4	Ms 7.5	Earthquake induced submarine landslide
Venezuela	10.60 (10.60)	64.50 (64.30)	1726		3		Earthquake
Venezuela	10.50 (10.50)	64.50 (64.30)	1750		3		Earthquake
Hispaniola	18.10 (18.30)	70.70 (70.70)	10/18/1751	1900 UT	4	Ms 7.3	Earthquake
Haiti	18.00 (18.40)	72.20 (72.80)	11/21/1751	0750 LT	3		Earthquake
Martinique and Barbados	14.40	61.00	4/24/1767	0600 UT	3		Shocks
Haiti	18.70 (18.60)	72.63 (72.80)	6/3/1770	1915 LT	4		Earthquake
Costa Rica	10.20	82.90	2/22/1798		4		Earthquake
Venezuela	11.50	66.90	3/26/1812		3		Earthquake

Table 1 (Continued)

Tsunami origin	Latitude (°N)	Longitude (°W)	Date	Time	Validity rating	Earthquake magnitude and corresponding scale	Source type and brief description
Jamaica	17.70 (18.00)	76.30 (76.50)	11/11/1812	1818 UT	3		Earthquake
Costa Rica, Nicaragua, and Panamá	9.60 (9.50)	82.20 (83.00)	5/8/1822	0500 UT	4	Ms 7.6	Earthquake
Martinique	14.40	61.00	11/30/1823	1130 LT	4		Earthquake
Martinique	14.20	61.10	11/30/1824	0330 LT	3		Earthquake
Trinidad and St. Christopher	12.40 (12.40)	-61.60 (61.50)	12/3/1831	1140 UT	4		Earthquake
Hispaniola and Cuba	19.97 (19.50)	72.10 (72.10)	5/7/1842	2200 UT	4	Ms 8.1	Earthquake (no effect in PR)
Guadeloupe	16.10	62.20	2/8/1843	1435 UT	4	Mw 8.3	Earthquake induced landslide
Cumaná, Venezuela	12.10	63.60	7/15/1853	1415 LT	3	Ms 6.7	Earthquake
Honduras	16.00 (16.20)	88.20 (88.50)	8/9/1856		4	Ms 7.5	Earthquake
St. Thomas, St. Croix, Puerto Rico, Dominica	18.10	65.10	11/18/1867	1850 UT	4	Ms 7.5	Earthquake; along the north scarp of the Anegada Trough; 15 to 20-km SW of St. Thomas; St. Croix, St. Thomas, and Isla de Vieques formed a triangle around the epicenter; others believe it may have been of volcanic origin on Little Saba

Table 1 (Continued)

Tsunami origin	Latitude (°N)	Longitude (°W)	Date	Time	Validity rating	Earthquake magnitude and corresponding scale	Source type and brief description
Puerto Rico	18.10	65.10	3/17/1868	1045 UT	4		Earthquake
Venezuela	10.80 (10.70)	63.80 (63.80)	8/13/1868	1137 LT	4		Earthquake
Lesser Antilles	15.50	61.50	3/11/1874	0430 LT	4		Earthquake
Jamaica	19.60	75.50	8/12/1881	0520 LT	4		Earthquake
Panama	10.00	79.00	9/7/1882	1418 UT	4	Ms 8.0	Earthquake (landslide?)
Haiti	19.70	74.40	9/23/1887	1200 UT	4		Earthquake
Venezuela	11.00	66.40	10/29/1900	0842 UT	4	Ms 8.4	Earthquake
Jamaica	18.50 (18.20)	76.60 (76.70)	1/14/1907	2030 UT	4	Ms 6.5	Earthquake induced submarine landslide
Puerto Rico	18.50	67.50	10/11/1918	1414 UT	4	Ms 8.25	Earthquake induced submarine landslide (subduction near the Bronson deep [Mona Canyon]; cables cut in several places)
Puerto Rico	18.50	67.50	10/24/1918	2343 LT	4		After shock from the 10/11/1918 earthquake
Cumaná, Venezuela	10.60	65.60	1/17/1929	1152 UT	4	Ms 6.9	Earthquake (fault activity; slides and collapses)
Cuba	19.50	75.50	2/3/1932	0616 UT	3	Ms 6.7	Earthquake
Hispaniola	19.30	68.90	8/4/1946	1751 UT	4	Ms 8.1	Earthquake

Table 1 (Continued)

Tsunami origin	Latitude (°N)	Longitude (°W)	Date	Time	Validity rating	Earthquake magnitude and corresponding scale	Source type and brief description
Puerto Rico	19.50	69.50	8/8/1946	1328 UT	4	Ms 7.9	2nd shock from 8/4/46 earthquake; this one located 100-km to the NW
Barbados, Antigua, Dominica	15.80	59.70	12/25/1969	2132 UT	4	Ms 7.7	Earthquake
Leeward Is.	17.00	62.40	3/16/1985	1454 UT	4	Ms 6.3	Earthquake (possible landslide)
Puerto Rico	19.23 (18.90)	68.77 (63.80)	11/1/1989	1025 UT	3	Ms 5.2	Earthquake
Costa Rica, Panama	9.90 (9.60)	82.60 (83.20)	4/22/1991	2156 UT	4	Ms 7.6	Earthquake
Venezuela	10.90 (10.60)	63.50 (63.50)	7/9/1997	1924 UT	3	Mw 7.0	Earthquake

Determination of IAS Tsunamigenic Potential

This study simulates events with the potential to have far-field (greater than 1000-km) destructive consequences and illustrates where impacts are possible. The proximity of the islands to each other makes it difficult for tsunami energy to propagate out of the region (or, in the case of origins outside of the region, to move into the Caribbean Sea). The tsunamigenic potential is an index that considers both the spatial frequency of tsunamigenic events and the geologic and tectonic regime of the region. This index helps identify where the next tsunamigenic event is likely to occur. In order to quantitatively measure the tsunamigenic potential of events it is necessary to place the data into bins. Through experimentation it was determined that 1° resolution is optimal because it is large enough to encompass more than one event but small enough to discern distinct geologic and tectonic areas.

The McCann [2006] tsunamigenic event source map (see Figure 1) is used to incorporate the geologic and tectonic regime of the region. Assigning a weighting system (Table 2) to the event source map, based on source type, allows it to be used as a relative tsunamigenic risk map. The weights, although subjective, allow for a quantification of the tsunamigenic event potential. High, medium, and low risk can be directly translated into weights (3, 2, and 1 respectively) but slow earthquake potential, plate bending, or platform deformation regions as well as active faults and geologic belts and ridges also increase the potential for a region to produce a tsunami and are therefore assigned a weight of 1.5. This tends to be more important where areas of high, medium, and low risk overlap these regions.

Table 2 – Weight assignments to the tsunamigenic event source map [*McCann*, 2006].

High risk	Medium risk	Low risk	Slow earthquake, belt or ridge, plate bending, platform deformation, active fault
3	2	1	1.5

The weight attributes of each source type are applied to the 1° resolution grid (Figure 3) and when a grid cell or bin is not completely covered by a source type, the fractional area each source type encompasses is calculated. This is multiplied by the weight of the source type to determine the weight of the bin. Multiple weight types in a single bin are combined in superadditive process. For example, if a bin contains 1/3 high risk, 1/5 slow earthquake, and 1/3 platform deformation the resulting weight is: $(1/3 * 3) + (1/5 * 1.5) + (1/3 * 1.5) = 1.8$. The fractional areas can be both greater than or less than 1 since source types overlap. The final value of each bin is calculated by adding the spatial frequency to the potential bin weights (Figure 4).
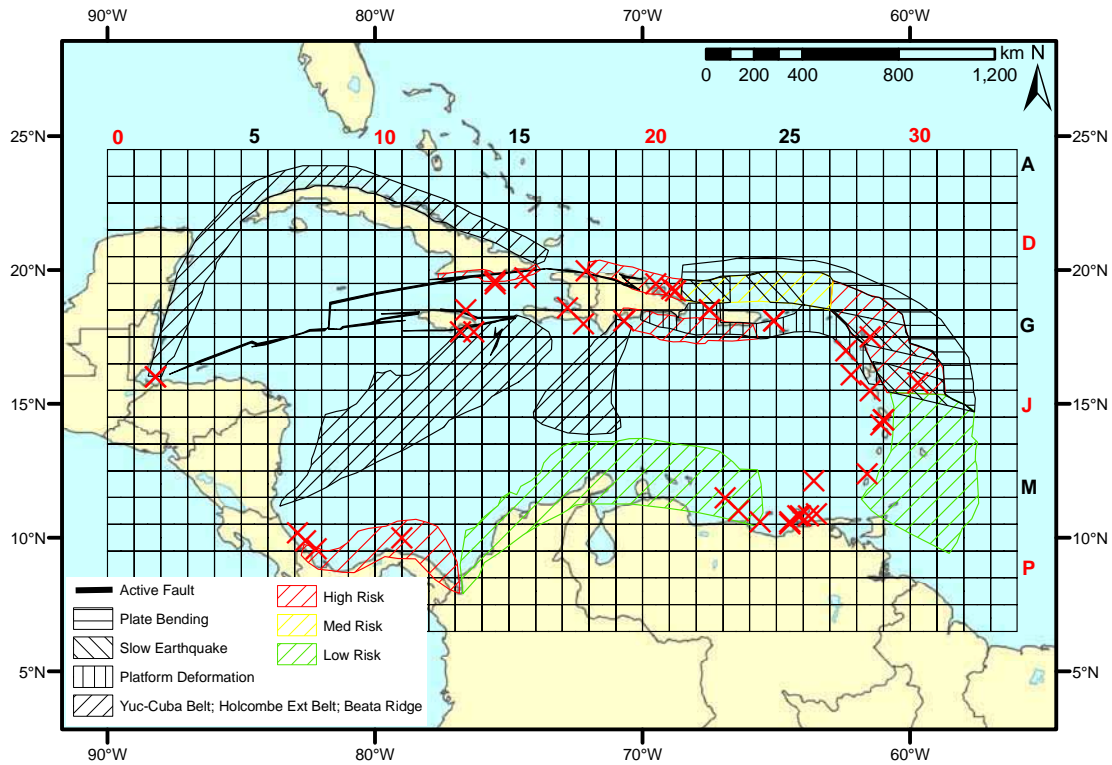
Figure 3 – 1° resolution grid, map of the IAS, historical tsunami origins, and tsunamigenic source regions. "X" represents the location of the historical origins.
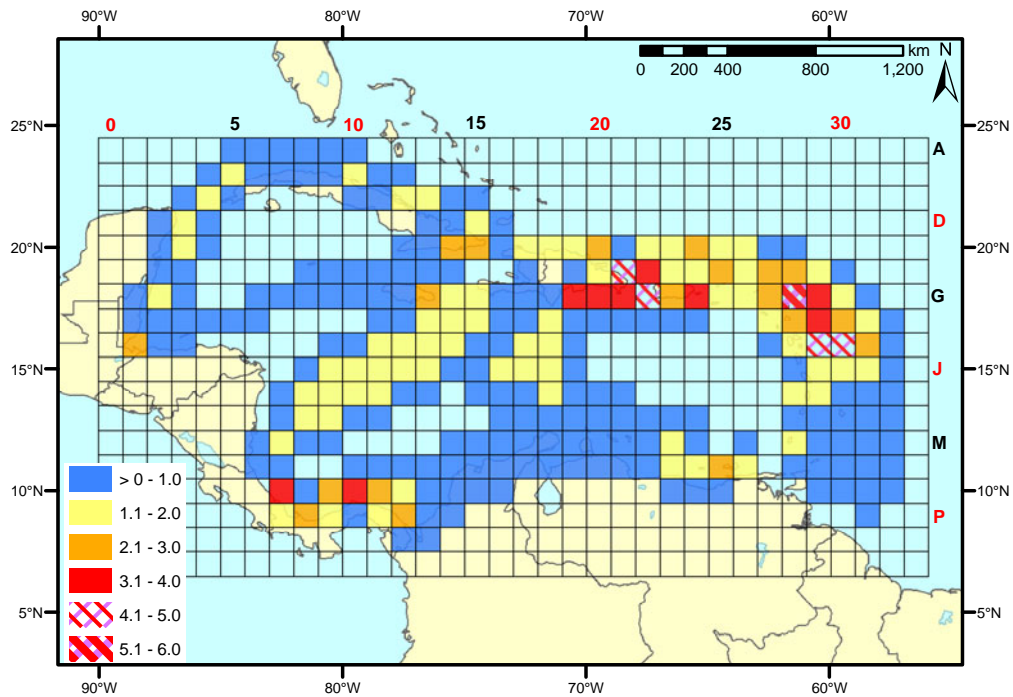

Figure 4 – Sector total weights. Result of binned historical tsunami origins and weight assignments to 1° resolution grid. Bins without coloring have a value of zero.

Modeling

A numerical simulation of the historic tsunamis helps explain tsunami propagation throughout the region, determine which coastlines are likely to be affected, and measure the travel time to those locations. Initial conditions (Table 3) are the same for every tsunami simulation due to a lack of specific historical data.

The NCOM is a three-dimensional model featuring flexibility of model grid discretization and numerical methods [*Martin*, 2000; *Morey, et al.*, 2003b; *Morey, et al.*, 2003a]. Other studies of historical tsunamis in the Caribbean have used different models but these are based on the same basic equations used by the NCOM [*Mader*, 2001; *Mercado and McCann*, 1998]. Some of the basic equations of motion that NCOM solves are listed here in Cartesian coordinates from Morey et al. [2003b] (Equations 1 – 4). Although the Coriolis term is accounted for in the NCOM, its contribution is relatively small given the simulation duration (6-hr).

$$\frac{\partial u}{\partial t} = -\nabla \bullet (\mathrm{V}u) + Qu + fv - \frac{1}{\rho_0}\frac{\partial p}{\partial x} + F_u + \frac{\partial}{\partial z}\left(K_M\frac{\partial u}{\partial z}\right) \tag{1}$$

$$\frac{\partial v}{\partial t} = -\nabla \bullet (\mathrm{V}v) + Qv + fu - \frac{1}{\rho_0}\frac{\partial p}{\partial y} + F_v + \frac{\partial}{\partial z}\left(K_M\frac{\partial v}{\partial z}\right) \tag{2}$$

$$\frac{\partial p}{\partial z} = -\rho g \tag{3}$$

$$\nabla \bullet \mathrm{v} = \frac{\partial u}{\partial x} + \frac{\partial v}{\partial y} + \frac{\partial w}{\partial z} = Q \tag{4}$$

$$\rho = \rho(T, S, z)$$

where,

u, v = velocity vector terms (m s^{-1}) ∇ = del operator   V = unit vector
Q = a volume source or sink term (m^3 s^{-1}) t = time (s) f = coriolis parameter
ρ_0 = reference water density (kg m^{-3}) p = pressure (Pa) S = salinity
F_u, F_v = friction vector terms (N) x, y, z = coordinate directions
T = potential temperature (^{o}C) g = gravitational acceleration (m s^{-2})
K_M = vertical eddy coefficient for momentum

A leap-frog, semi-implicit time stepping integration scheme is used for the tsunami simulations. This allows the use of larger time steps while maintaining stability and accuracy [*Morey, et al.*, 2003b; *Rueda and Schladow*, 2002]. However, if too large a time step is used and the Courant, Friedrichs, and Lewy (CFL) condition is violated, gravity waves (such as those modeled for this research) may be slowed down [*Bartello and Thomas*, 1996; *Dupont*, 2001]. The CFL condition states that the time step must be smaller than the time it takes for a wave to propagate from one grid point to the next (Equation 5).

$$C < 1$$
$$C = \frac{c\Delta t}{\Delta x}$$
(5)

where, c = wave celerity (m s^{-1}); Δt = time step (s); and Δx = grid space (m)

Although it is a three-dimensional model, for these simulations the NCOM is run as a barotropic model with one depth-averaged vertical grid cell. Tidal components are not included and the temperature and salinity remain constant. All tsunamis are assumed to be shallow water waves. Sea boundaries are open and allow perturbations to radiate out of the model domain. Land boundaries are closed and act as vertical walls with heights equal to the adjacent ocean grid cell depth (typically 4-m). Land elevation is set to 20-m above sea level, and to avoid dry cell conditions as a wave reaches the coast, the minimum water depth is set to 4-m. Wave run-up on land is outside the scope of this study due to a lack of high resolution bottom and coastal topography for the study area, and a lack of high quality historical observations/measurements to ground truth model results. The grid resolution is set to 2-arc-minutes to match the resolution of the ETOPO2 [*NGDC*, 2001] global bathymetric and topographic dataset, which is used as the model bottom topography.

Initial Conditions

Known as an inverse tsunami problem, a method of determining some of the initial conditions for a tsunamigenic event is to back-calculate them from historical observations of tsunami impacts [*Mader*, 2001; *Murty*, 1977]. However, the historical record for tsunamis in the Caribbean region is poor and it is difficult to reconstruct such events with any accuracy. Some works have used a seismic or initial condition model [*Mercado and McCann*, 1998; *Meyer and Caicedo O.*, 1998] to determine the initial wave parameters while other models such as NCOM and MOST (Method of Splitting Tsunamis) can also run with user-defined initial conditions. For this study, several sensitivity tests were run to determine initial wave amplitude and e-folding radius, bottom roughness height, model time step, surface field output interval, and total run time. Results are summarized in Table 3.

Table 3 – Sensitivity test results summary

Initial amplitude (m)	e-folding radius (m)	Bottom roughness height (m)	Time step (s)	Surface field output interval (s)	Total run time (hr)
4	10,000	0.003	7.5	45	6

The surface field output interval depends on the temporal resolution required to consistently identify the exact moment of tsunami impact. A surface field output interval of 45-sec was sufficient to obtain adequate temporal resolution. The sensitivity experiments converged on a model time-step of 7.5-sec and a grid spacing of 2-arc-minutes, which also satisfies the CFL condition (see Equation 5). Based on a celerity of 222 m s^{-1} (~ 800 km hr^{-1}), two time steps will pass as a wave moves from one grid point to another.

The shape of the initial wave adds the most uncertainty to the results of the simulations presented here. However, too little is known about the initial conditions of all of the events simulated. Therefore, in order to compare the output from each model run, the same initial conditions are used to initialize all of the historical tsunami simulations. Zahibo et al. [2003b] has also used the same initial conditions for 19 historical events, and a time step and grid spacing of 6-sec and 3000-m, respectively.

Each tsunami is modeled as a point source using a normalized Gaussian dome with an amplitude of 4-m and an e-folding radius of 10,000-m (see Table 3; Equations 6 – 11). This assumes that the entire water column is composed of an incompressible fluid and that the tsunami-genesis process is instantaneous [*Okada*, 1985]. This assumption is based on previous works such as Kowalik and Whitmore [1991], Shuto [1991], and Mercado and McCann [1998].

The initial shape of the sea surface η is given by,

$$\eta(r) = A * e^{\left(\frac{-r^2}{2*R^2}\right)} \tag{6}$$

where, A is the initial maximum height of the wave above a resting sea surface (m); R is the e-folding radius (m); and r is the radius from the center of the perturbation (m). Given the location for the center of the initial perturbation, $\eta(r)$ can be readily mapped onto the ocean model grid space.

Determination of Coastal Grid Points (CGP), Population Data Integration, and Time Series Analysis

Analyses of population data within the model study region are conducted to determine the approximate population densities along the coastlines. In the model, 10,623 grid points adjacent to land are identified in an area approximately from 7ºN, 59ºW to 36ºN, 98º W (Figure 5A). A close up of CGP's around Puerto Rico illustrates resolution (Figure 5B). Population data is obtained from the Latin American and Caribbean Population Database (LACPD) [*CIAT, et al.*, 2005]. This database encompasses the Caribbean and South and Central American regions at a mean resolution of 33,000-m. The resolution varies from country to country and is generally 9,000- to 53,000-m. Each CGP is assigned the value of the LACPD population cell closest to it.

Figure 5A – All 10,623 coastal grid points used in the initial time series analysis study.
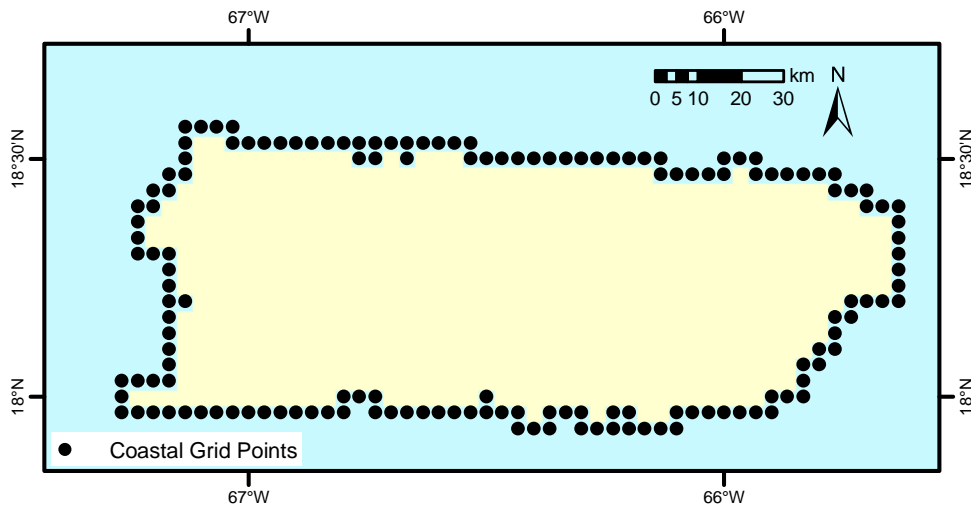

Figure 5B – Inset of figure 5A; Close-up view of CGPs around Puerto Rico

The CGP's bordering the continental United States are not used because, as it is shown later (see Results and Discussion), the travel time to where the continental US is impacted by the simulated tsunamis is at least 4-hr (Figure 6). Sea level gauges throughout the Caribbean would identify the threat of a destructive tsunami impact along the continental US with at least 3-hr of warning time eliminating the need to analyze those CGP's for this part of the study.

Figure 6 – Locations of the 8009 CGP's with population data attributes. The CGP's bordering the continental United States seen in figure 5A are not shown here.

Efficient use of a limited number of sea level gauges requires that each gauge warn the greatest number of people possible. This is achieved through the use of population centers. A population center, due to the high and variable resolution of the population data set, is defined as a CGP having a population of over 500. Once these points are identified, the dataset is edited to eliminate replicates and points in close proximity to each other. It is necessary to supplement this list with major tourist locations since these do not necessarily have high populations. The resulting dataset is summarized in table 4 and displayed in figure 7.

Table 4 – List of population centers. * denotes added tourist location; Coordinates from www.fallingrain.com and adjusted to nearest CGP.

St. Johns, Antigua and Barbuda*	Near Old Harbour, Jamaica
Basseterre, Saint Kitts and Nevis*	Kingston, Jamaica
Basse-Terre, Guadeloupe (France)*	Ponce, Puerto Rico
Christiansted, St. Croix (Virgin Islands)*	Les Cayes, Haiti
Marigot, Sint Maarten (Neth. Ant.)*	Mayagüez, Puerto Rico
Roseau, Dominica*	Fajardo, Puerto Rico
Fort-de-France, Martinique (France)*	Santo Domingo, Dominican Republic
Castries, St. Lucia*	Near Jeremie, Haiti
Bridgetown, Barbados*	Near St. Marc, Haiti

Table 4 (Continued)

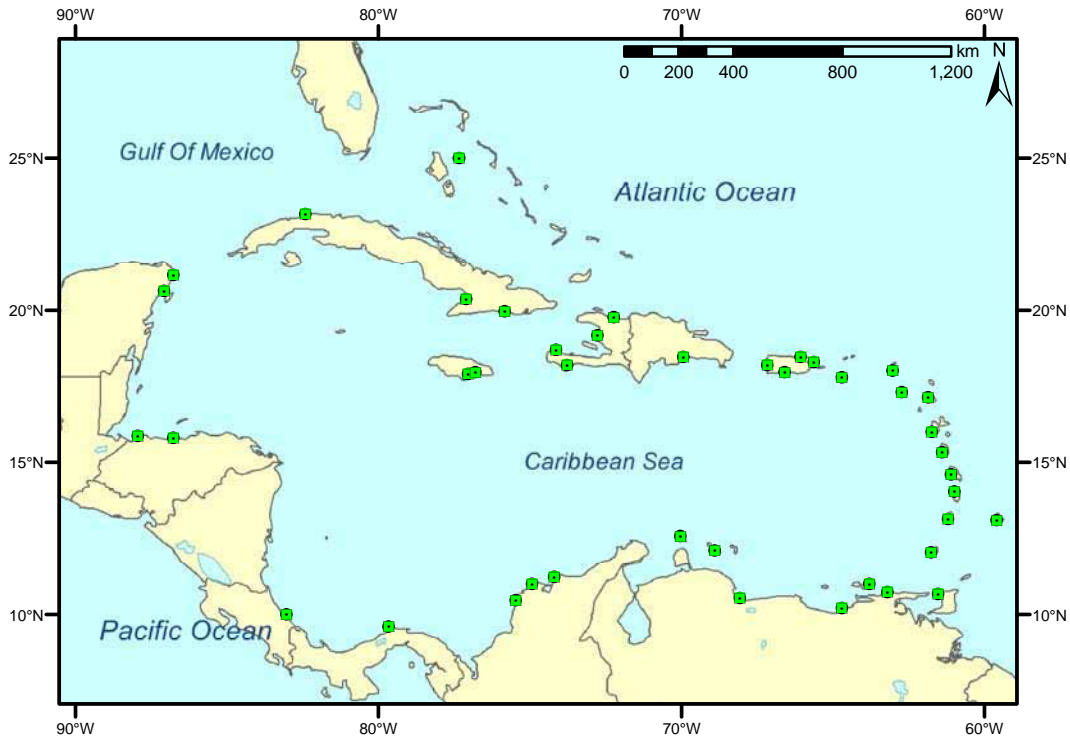|	
Kingstown, St. Vincent and the Grenadines*	Cap-Haïtien, Haiti
St. George's, Grenada*	Santiago De Cuba, Cuba
Puerto Limon, Costa Rica*	South Beach, Bahamas (New Providence)
Portobelo, Panama*	Near Barcelona, Venezuela
Cancun, Mexico*	Near Puerto Cabello, Venezuela
Playa del Carmen, Mexico*	Near Carúpano, Venezuela
Willemstad, Curaçao*	Pampatar, Venezuela
Cartagena, Colombia	La Ceiba, Honduras
Barranquilla, Colombia	San Juan, Puerto Rico
Santa Marta, Colombia	Port-of-Spain, Trinidad and Tobago
near Oranjestad, Aruba	Havana, Cuba
Puerto Cortes, Honduras	Manzanillo, Cuba

Figure 7 – Population centers (represented by the squares).

A time series of model sea level are extracted for each CGP, and from them, tsunami travel time is calculated. A CGP is determined to have been impacted by the tsunami if the criterion

$$(\eta_n - \eta_{n-2})^2 > 10^{-5} \, \text{m}^2 \tag{7}$$

is met, where n is any output record number (at 45-sec intervals). Condition (7) is true when the time rate of change of the sea level at a CGP exceeds some threshold. Travel time is defined as the

time between the model initialization and the time when the first peak or trough above the threshold reaches the CGP. Both peaks and troughs are considered to determine travel time because, due to the initial condition uncertainty, phase error may be present. A peak or trough is identified when the time series meets the criteria set forth in both (7) and the condition

$$\frac{\eta_{m+1} - \eta_m}{\eta_m - \eta_{m-1}} < 0 \tag{8}$$

where, m is any output record number (at 45-sec intervals).

Sea Level Gauge Location Determination

       A sea level gauge for a TWS should be positioned to maximize warning time. Several factors such as population centers, locations where a tsunami may occur, travel time or propagation speed, and wave dissipation are considered when calculating warning time. The first Pacific Ocean DART buoy detection array was designed to detect a tsunami within 30-min after the generating earthquake [*Bernard, et al.*, 2001]. The IAS TWS proposal, accepted by the IOC (Intergovernmental Oceanographic Commission), recommends at least 15-min of warning time [*IOC-UNESCO*, 2005]. This study calculates warning time by subtracting travel time to the population center from the travel time to a sea level gauge. A population center is considered warned if it can be notified within 30-min after tsunami generation. In general, the closer the gauge is to the tsunami origin, the more warning time available to population centers.

       Knowing where a tsunami will originate is essential to determining where a gauge should be installed. The McCann [2006] tsunamigenic source map, used in part to create the tsunamigenic risk map (Figure 4), appears to have a gap in a tsunami risk region just north of Venezuela in sectors N25 and N26 (Figure 3). Based on McCann's methodology for classifying risk or source areas, and the frequency of historical tsunamis occurring in those sectors, they should be within a region of low risk. This additional low risk value is added to the value of sectors N25 and N26 as if completely covered by a low risk area. The rest of the bins or sectors without values are discarded and the upper ~ 5%, or 15 of the remaining sectors are considered to be where tsunami-genesis risk is relatively highest (Figure 8).
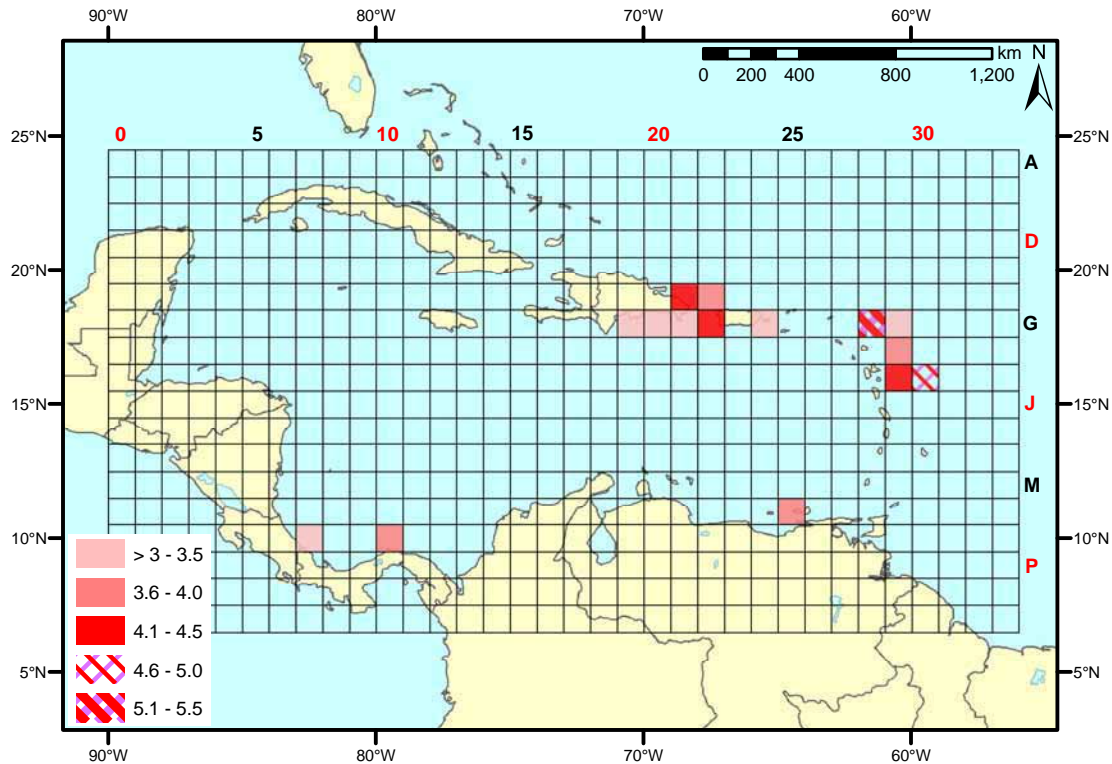
Figure 8 – Top 5% of risk sectors. The color bar shown here is different than that shown in figure 4.

Travel time is measured from the center of the shaded sectors in Figure 8 to the nearest point of land and to the population centers using a series of isochrones. The recommended gauge location corresponds to the point of land nearest to the center of the relatively higher risk tsunamigenic sectors. With this strategy, each point closest to a high-risk sector should receive a sea level gauge resulting in 15 locations. However, some sectors are closest to the same point of land and the final number of locations identified is discussed later. For simplicity, gauge locations are referred to as the sector they correspond to.

Location Priority for Coastal Sea Level Gauges
    Through an iterative experimental process a simple decision matrix is developed to evaluate the relatively highest risk sectors in the following categories:
  i.   Sector risk value
  ii. Number of population centers the sector's gauge can warn in time
  iii. Number of population centers less than 1000-km away
  iv. Number of sectors closest to one potential gauge location
  v.   Number of sectors sharing a border
Each sector is assigned a rank in all categories, the ranks are added together, and the sector with the lowest number is assigned an overall rank of 1, the second lowest a rank of 2, etc. The final priority list includes all aspects with equal consideration since all ranks are simply added together.

The sector risk values are ranked so the sector with the highest relative risk receives first priority. This means that, to a first order, a sea level gauge is most useful within or nearest to a sector that is the most likely to generate a tsunami. This location, though, may not be able to warn as many population centers as another, reducing its effectiveness.

According to the warning time criteria of 30-min, each location has the potential to warn a certain number of population centers. However, in the Caribbean, the risk to population centers is low if they are at least 1000-km away from the tsunami origin [*Zahibo, et al.*, 2003b]. A direct line distance is used in this study, since the resulting complex island reflections and refractions soon after tsunami generation make it difficult to perform accurate ray tracing. The list of population centers each gauge can warn is reduced to those less than or equal to approximately 1000-km away from the center of the sector. The sector and corresponding gauge that warns the most population centers less than or equal to approximately 1000-km away is given higher priority.

In some cases, different risk sectors are closest to the same point of land (Figure 10). It is more efficient to install a sea level gauge on a point of land closest to more than one sector. This gives the gauge the ability to warn of a tsunami originating from multiple sectors. Higher priority is allocated to sectors that share a gauge location.

Population centers near multiple higher risk sectors have increased potential to be impacted by a tsunami. To account for this sector density or clusters of higher risk sectors, the number of borders each sector shares with another sector is counted. In this manner, higher priority is skewed towards the clusters of risk centers.

RESULTS and DISCUSSION

Our systematic approach to assess sea level gauge location and priority should assist in developing an IAS TWS. Here we review the modeling decisions and results, vulnerability of the IAS coastline to tsunami impact, sea level gauge installation location and priority, and currently operational sea level gauges within the IAS.

Modeling Validity

Major aspects of modeling include choosing the correct model, the accuracy of the initial conditions, and the validity of assumptions. Depending on the model used for both propagation and initial displacement there may be differences in calculated wave amplitudes. However, previous studies have not evaluated whether the choice of model affects travel time estimates [*Mercado and McCann*, 1998; *Whitmore*, 2003; *Zahibo, et al.*, 2003a]. Travel times estimated here, in general agree with those calculated in both Weissert [1990] and Mercado and McCann [1998] and observed by Reid and Taber [1919].

Weissert [1990] developed an isochron time chart for the 1867 Virgin Islands tsunami (see Table 1). Travel times are in reasonable agreement for open areas, but less in regions of more complicated bottom topography. For example, he estimated a travel time of 100- to 120-min to the Northeast coast of Cuba, but the NCOM travel time calculation was approximately 250- to 350-min. This significant difference may have been a result of a coarser bottom topography used in Weisserts' study (ETOPO5), or the breakdown of that model's ability to simulate a tsunami in shallow water, as explained by the author.

Mercado and McCann [1998] simulated the 1918 Puerto Rico tsunami (see Table 1) and show a sea level time series for three Puerto Rico locations: Aguadilla, Mayagüez, and Boquerón.

These three time series are compared to those generated from the NCOM output. As in this study, travel time to these locations is taken as the time corresponding to the first peak or trough on the Mercado and McCann [1998] sea surface elevation time series. Reid and Taber [1919] report observations of the 1918 Puerto Rico tsunami. The travel times they and Mercado and McCann [1998] report generally agree with those produced in this study.

Any discrepancies with Mercado and McCann [1998] may be because they use a higher bathymetric and grid resolution, more accurate bottom topography, and run-up capability (Mercado and McCann use a 3-arc-second grid resolution where a 2-arc-minute resolution is used in this study). In addition, the location and shape of the initial wave is also different. They generate the tsunami along a multi-segment fault line whereas it is considered a point source here.

Tsunami Travel Time and IAS Coastline Vulnerability

Based on the temporal frequency of historical tsunamigenic events, the IAS region is likely to experience another destructive tsunami at any moment [*O'Loughlin and Lander*, 2003; *Pararas-Carayannis*, 2004; *Zahibo, et al.*, 2003b; *Zahibo, et al.*, 2003a]. Several works have discussed the local nature of devastating effects from many historical tsunamis [*Mercado and McCann*, 1998; *Meyer and Caicedo O.*, 1998; *Pararas-Carayannis*, 2004; *Zahibo, et al.*, 2003a]. It has also been shown that tsunamis generated in the Caribbean can be destructive as far away as 2- to 3-hr [*Zahibo, et al.*, 2003b]. In order to determine the IAS coastline vulnerability, here it is assumed that these tsunamis can be destructive up to 6-hr away.

Figure 9 displays where 42 historical tsunamis have had the potential to impact (based on the model experiments), and indicates the frequency of impact at those locations. To show where the continental United States has had the potential to be impacted, all 10,623 CGP's are included in figures 9 – 11. Some areas are never hit and some are hit by every tsunami modeled. The two main factors controlling this are the origin location and bottom topography. To incorporate travel time with impact frequency, the mean travel time is displayed in Figure 10. It can be inferred that where the mean travel time is low (≤30-min), the majority of tsunamis impacting that location originated close to it. The opposite can be inferred where the mean travel time is high (>1.5-hr).

The median travel time helps understand what locations may be more vulnerable to a regional tsunami regardless of impact frequency (Figure 11). Compared to mean travel time, the median tends to be lower at locations that are hit more frequently. The mean travel time is longer than the median 64% of the time, suggesting that there are more locations that are hit more often from tsunamis that travel long distances. This is an indication of their vulnerability to regional tsunami impact.
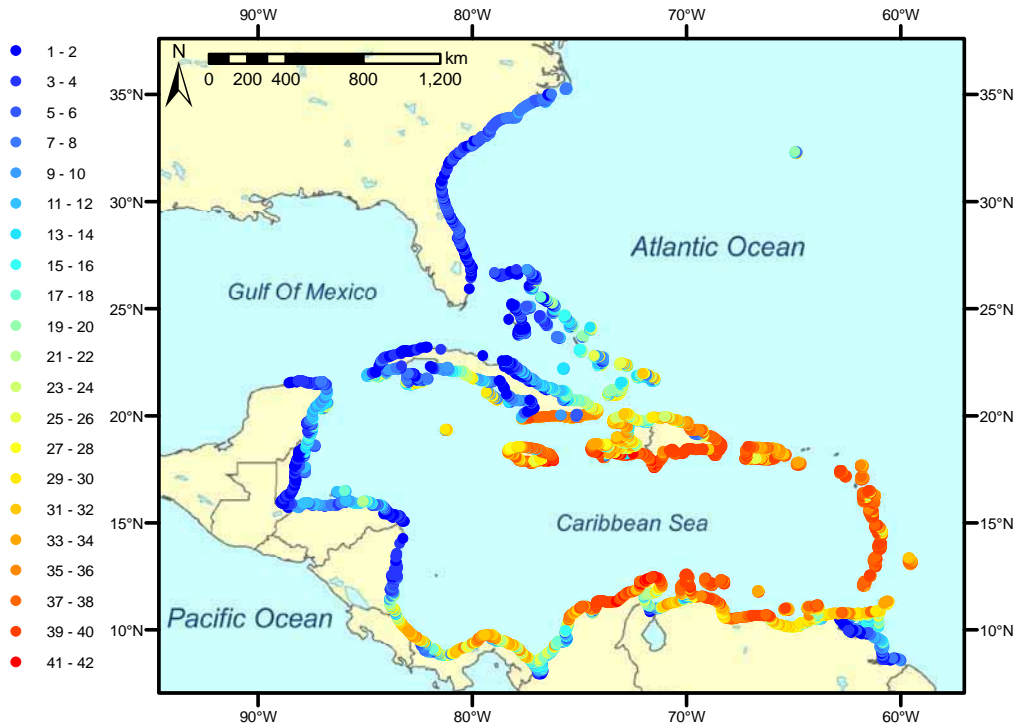
Figure 9 – Impact frequency. Locations where a CGP was impacted by at least one of the 42 historical tsunamis. Colors denote frequency of impact at that location.
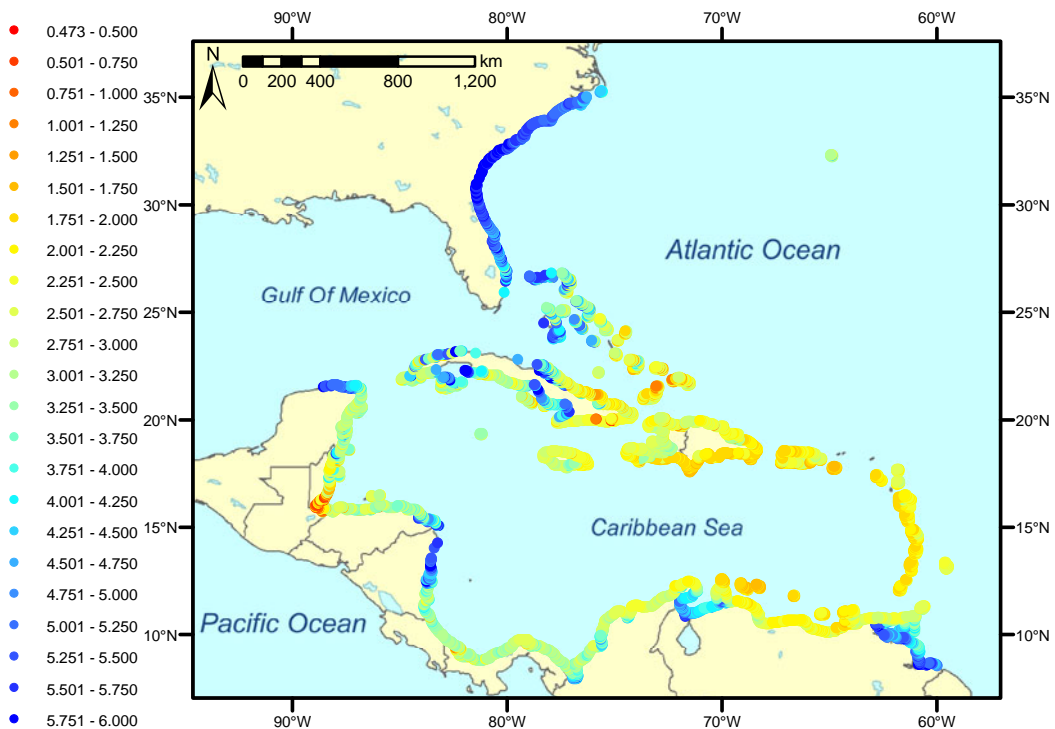

Figure 10 – Mean travel time. Similar to figure 9 but here colors denote mean travel time in hr to that location.
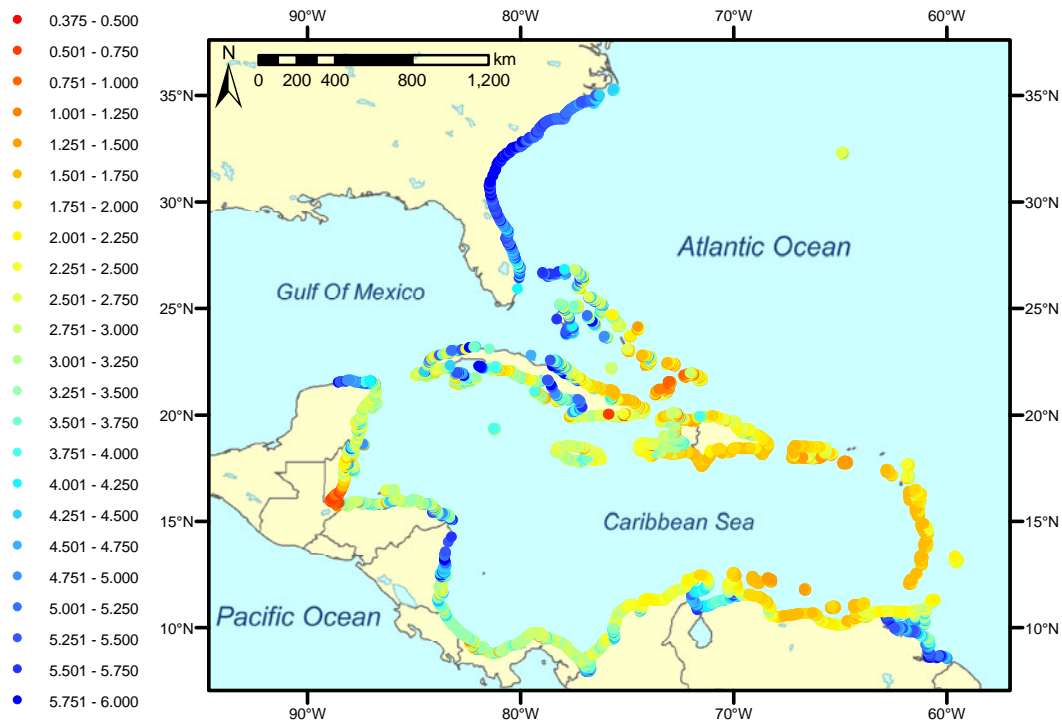
Figure 11 – Median travel time. Similar to figure 9 but here colors denote median travel time in hr to that location.

Sea Level Gauge Location Priority

This study uses a two-pronged approach to determine the IAS regional tsunami risk. One assumes that a tsunami impact has the potential for destruction up to 6-hr from the origin and the other assumes that a tsunami will only be destructive within approximately 1000-km from the origin. The former is important when determining what locations have historically had the potential for impact and the latter is considered when optimizing and prioritizing gauge locations.

Table 5 summarizes the rank of the higher risk sectors by the factors dictating the installation location priority. These factor ranks are combined in a linear fashion to determine an overall rank (Table 6). In the event two sectors have the same value, they are assigned the same rank. The gauge corresponding to the sector with the highest overall rank should be installed first. The insertion of the low risk area over sectors N25 and N26 described in Methods ("Sea Level Gauge Location Determination") led to the addition of sector N25 to the list of relatively higher risk sectors.

Table 6 shows the prioritized list of initial locations for sea level gauges recommended to provide an efficient warning system. When two sectors share the same potential gauge location and have a different priority, the higher priority rank is applied to both sectors. Several sectors share priority and two different locations are recommended for sector G22. Priority sharing can be resolved in a number of ways. The importance of one factor can be increased or decreased, a multiplier can be applied to a factor, or other factors can be included in the decision matrix such as site infrastructure, security of a site, and maintainability. As explained earlier, this study assesses regional tsunami risk of impact based on historical tsunamigenic events, the geologic and tectonic regime of the region, wave propagation dynamics, and the location of major population centers

within a range of 1000-km from the center of the higher risk sectors. Nonetheless, a complete warning system should also consider exactly where run-up and inundation would occur and to what extent.

Table 5 – Decision rank matrix. The sectors are arranged in alphabetical order.

Sector	Risk value	# of sectors with same closest land	# of higher risk sectors sharing a border with another higher risk sector	# warned < 1000- km away	Total
F21	5	3	1	2	11
F22	8	3	1	5	17
G19	15	3	2	4	24
G20	13	3	1	1	18
G21	11	3	1	3	18
G22	3	3	2	4	12
G24	14	3	3	6	26
G28	1	2	2	8	13
G29	12	2	1	9	24
H29	9	1	1	10	21
I29	4	1	1	8	14
I30	2	1	2	11	16
N25	6	3	3	7	19
O7	10	3	3	12	28
O10	7	3	3	12	25

Table 6 – List of initial sea level gauge locations recommended for a TWS. Locations listed in order of highest to lowest priority groups. Coordinates should only be used as a guideline.

Sector	Approximate location for gauge installation	Priority
F21	Arena Gorda, Dominican Republic (18.78°N, 68.52°W)	1
G22	Isla Mona, Puerto Rico (18.09°N, 67.89°W) or Boquerón, Puerto Rico (18.02°N, 67.17°W)	2
G28, G29	Barbuda (17.64°N, 61.80°W)	3
H29, I29, I30	La Désirade, Guadeloupe (16.32°N, 61.05°W)	4
F22	Aguadilla, Puerto Rico (18.50°N, 67.15°W)	5
G20 G21	Boca Chica, Dominican Republic (18.45°N, 69.61°W) Isla Saona, Dominican Republic (18.11°N, 68.57°W)	6
N25	Punta Arenas, Venezuela (10.97°N, 64.4°W)	7
G19	Las Calderas, Dominican Republic (18.20°N, 70.5°W)	8
O10	Portobelo, Panamá (9.55°N, 79.65°W)	9
G24	Isla de Vieques, Puerto Rico (18.10°N, 65.45°W)	10
O7	Punta Manzanillo, Costa Rica (9.63°N, 82.64°W)	11

Changing the number and location of population centers, as well as the decision criteria, may affect the suggested gauge priority. The population centers are selected based on population

and tourism alone and may not need to be warned if they are protected by a wide continental shelf or other wave energy dissipation medium. In addition, the number of warnable population centers will increase if tsunamis have destructive capability at distances greater than 1000-km. Answers to these possibilities require higher resolution bottom topography, modeling more origins (including those that are hypothetical in areas of higher tsunamigenic potential), as well as calculating run-up and inundation.

The installation location coordinates depend on where the center of the higher risk sectors are and should therefore only be used as a guideline. The locations selected are based on the top 5% of the relatively higher risk sectors and do not constitute a finite list. Additional areas should be considered for sea level gauge installations, including Venezuela near the west coast of Margarita Island, the southeast coast of Jamaica, and the southeast coast of Cuba.

Although table 6 lists only one location per sector, in some cases two or three sensors may be more effective. It may take only one gauge to determine if the seismic event caused a tsunami, but this is a binary approach. It may not give enough information as to where else and to what extent the tsunami may impact on a larger scale. More sea level gauges can be used to detect a tsunami originating on either side of an island, and/or also improve travel time and wave height predictions.

A more general approach to a warning system is the installation of DART buoys. They have the potential to yield better predictions because, unlike a coastal sea level gauge, they receive a tsunami signal without being compromised by local effects or coastal noise. Although a DART buoy may prove more useful in propagation and wave height prediction as well as cover a larger origin area, they may not provide as much warning time. This approach cannot warn locations that are the same distance from the tsunami origin as the buoy, because a tsunami will reach both locations at about the same time. This reduces their usefulness and requires that a robust warning system employ a combination of both coastal and open ocean sea level gauges.

Operational Sea Level Gauges in the Caribbean

Figures 12a and b show the locations of some of the fully operational and proposed gauges as well as the recommended locations seen in table 6. The IAS TWS proposal [*IOC-UNESCO*, 2005] recommends that 31 sea level stations become tsunami ready to operate within the IAS TWS. The PRSN group has begun installing ten sea level gauges [*von Hillebrandt-Andrade*, 2006, personal correspondence]. A base station located in Mayagüez, Puerto Rico, will be capable of processing data from these and other sea level stations throughout the IAS. The NOAA National Ocean Service (NOS) has seven sea level gauges installed throughout Puerto Rico and the US Virgin Islands. Two of the PRSN tsunami ready gauges (Aguadilla and Isla Mona) and one of the NOAA NOS gauges (9752695) coincide with locations recommended by this study.

Any sea level gauges used for tsunami warning must be supported as a part of an operational system and regularly maintained. Support can come from a variety of sources because coastal sea level gauges are typically a component of a larger station capable of collecting various other data including wind speed and direction, relativity humidity, air temperature, water temperature, barometric pressure, precipitation, salinity, dissolved oxygen, water clarity, solar radiation, and current flow. These stations therefore have many applications, such as storm surge warnings and studies, hurricane forecasting, geostrophic current analysis, land subsidence, plate tectonics, commercial and recreational fishing and diving, search and rescue operations, and commercial shipping.
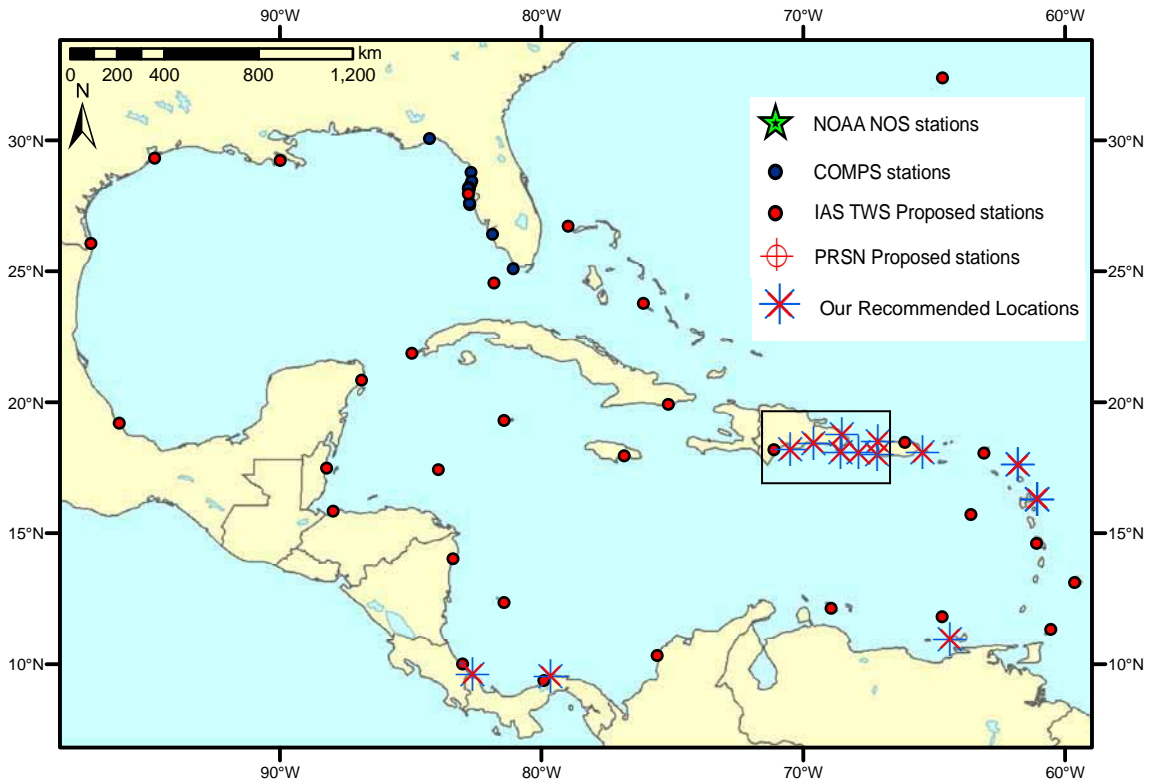
Figure 12a – Selection of operational and recommended sea level gauge stations in the IAS. There are 12 operational sea level gauges sponsored by the NOAA NOS, 13 locations for sea level gauges recommended by this study, 31 IAS TWS proposed locations, 10 PRSN locations proposed for the Puerto Rico Tsunami Ready Tide Gauge Network, as well as 11 Coastal Ocean Monitoring and Prediction System (COMPS) gauges shown in the figure. The alternate location for sector G22 is also shown. Box in northern Caribbean is enlarged in figure 12b.

Figure 12b – Inset of figure 12a; Close up view of stations around PR, the USVI, and the Dominican Republic. Illustrates the proximity of the locations recommended in this study with those already installed by NOS and those recommended by the PRSN.

CONCLUSIONS and RECOMMENDATIONS

The goal of a TWS is to mitigate loss of life and property caused by a tsunami. Different types of systems/networks are currently being successfully employed to measure, record, and telemeter both oceanographic and meteorological data for tsunami warning. This study determined prioritized locations for coastal sea level gauges in the IAS based on tsunami generation risk factors, tsunami propagation throughout the region, population distribution, and tsunami travel time to population centers. These locations will give the maximum warning time to the largest number of people in the most efficient manner.

A database of all sea level gauges installed or thought to be installed was compiled and used to coordinate the recommended locations. The expansion of the IAS regional tsunamigenic event risk analysis was accomplished by combining the spatial frequency of 42 historical tsunamis with a modified tsunami source map from McCann [2006]. This study assumes that the 42 tsunamis were generated by either a dip/slip earthquake or massive slide/slump and were regionally destructive. Each historical tsunami was modeled with the NCOM to show which coastal locations could have been affected by historical tsunamis and to estimate the respective travel times. Animations of select simulations are available at http://imars.usf.edu/tsunami/. Throughout this work a GIS database was created which will also be useful to those planning the IAS tsunami warning system.

This study established that, initially, 12 sea level gauges are recommended, and 3 of these locations already have or are planned to have a gauge. These locations correspond to the land closest to the center of the relatively higher risk sectors and should serve as a guide for installation. The list provided in Table 6 is not all-encompassing, but represents a start and will primarily warn against tsunamis that originate in the higher risk sectors. To determine exactly where a sea level gauge should be installed a thorough site evaluation is necessary. During the site evaluation, factors that need to be considered are those such as access to open water, proximity to a reef or other shoaling feature, infrastructure and security of site, and ease of station installation and maintenance.

It is difficult to predict where a tsunami will occur and how much damage it will do. Quantifying damage prediction for affected areas requires a better understanding of tsunamigenic event origins, higher resolution bottom topography, propagation modeling in the littoral zone, and inundation mapping. Run-up and/or inundation calculations must be performed for areas most susceptible to tsunami impact (see Figures 9 – 11). Mercado and McCann [1998] have begun doing this for Puerto Rico and this is already a viable product for areas around the Pacific at the Pacific Tsunami Warning Center [*Titov, et al.*, 2001].

Sea level gauges are a part of a larger system that records, processes, and telemeters data. These stations can provide meteorological and oceanographic data to support other projects such as hurricane and storm surge monitoring and prediction, climate change monitoring, and assist in improving numerical models [*Alverson*, 2005]. These types of systems in other areas around the US are already used by harbor pilots, ship captains, the U.S. Coast Guard, recreational and commercial divers and fishermen, the surfing and sailing industry, scientists, and the general public. Therefore, to guarantee continued existence and viability, these stations must have a multi-mission purpose to garner multifaceted support because thankfully, tsunamis do not occur very often.

REFERENCES

Air-Sea Monitoring Systems (2006), Assessment and restoration of the MACC sea-level monitoring stations travel report. (http://www.air-seasystems.com/macc/Sea%20Level%20Monitoring %20Stations%20Assesment%20Report.pdf)

Alverson, K. (2005), Watching over the world's oceans, *Nature*, *434*, 19-20.

Bartello, P., and S. J. Thomas (1996), The cost-effectiveness of semi-Lagrangian advection, *Monthly Weather Review*, *124*, 2883-2897.

Bernard, E. N., et al. (2001), Early detection and real-time reporting of deep-ocean tsunamis, paper presented at International Tsunami Symposium, Seattle Washington.

Bilek, S. L., and T. Lay (2002), Tsunami earthquakes possibly widespread manifestations of frictional conditional stability, *Geophysical Research Letters*, *29*, 1673.

Bird, P. (2003), An updated digital model of plate boundaries, *Geochemistry, Geophysics, Geosystems*, *4*, 1027-1079.

Bryant, E.A. (2005), *Natural Hazards*, 2nd ed., 312 pp., Cambridge Univ. Press, Cambridge, New York, Melbourne.

CIAT, et al. (2005), Latin American and Caribbean Population Database, Version 3, Centro Internacional de Agricultura Tropical (CIAT).

Curtis, G. D. (2001), A multi-sensor research program to improve tsunami forecasting, paper presented at International Tsunami Symposium, Seattle, Washington.

Demets, C. (1993), Earthquake slip vectors and estimates of present-day plate motions, *Journal of Geophysical Research*, *98*, 6703-6714.

Dunbar, P. (2005), Personal Correspondence, National Geophysical Data Center (NGDC). National Oceanic and Atmospheric Administration (NOAA)/ National Environmental Satellite, Data, and Information Service (NESDIS).

Dupont, F. (2001), Comparison of numerical methods for modeling ocean circulation in basins with irregular coasts, Dissertation thesis, McGill University, Montreal.

Fryer, G. J., and P. Watts (2000), The 1946 Unimak tsunami: Near-source modeling confirms a landslide, *EOS, Transactions, American Geophysical Union*, *81*, 748.

Fryer, G. J., et al. (2001), Source of the tsunami of 1 April 1946: A landslide in the upper Aleutian Forearc, in *Prediction of underwater landslide hazards*, edited by P. Watts, et al., Balkema, Rotterdam.

Grilli, S. T., and P. Watts (2005), Tsunami Generation by Submarine Mass Failure. I: Modeling, Experimental Validation, and Sensitivity Analyses, *J. Waterway, Port, Coastal, and Ocean Engineering*, *131*, 15.

Grindlay, N. R., et al. (2005), High risk of tsunami in the northern Caribbean, *EOS, Transactions, American Geophysical Union*, *86*, 121, 126.

Henson, J. I. (2006), Strategic Geographic Positioning of Sea Level Gauges to Aid in Early Detection of Tsunamis in the Intra-Americas Sea, Masters thesis, 68 pp, University of South Florida, St. Petersburg.

Henson, J. I., and D. Wilson (2005), Preliminary status report on tide gauges and observing stations in the Caribbean and adjacent waters, paper presented at The Group of Experts on the Global Sea Level Observing System (GLOSS) ninth session, IOC UNESCO, Paris, France, 24 − 25 February.

Hwang, L., and A. C. Lin (1969), Experimental investigations of wave run-up under the influence of local geometry., in *Tsunamis in the Pacific Ocean*, edited by W. M. Adams, pp. 407-425, East-West Centre Press, Honolulu.

IOC-UNESCO (2005), An Intra-Americas Sea Tsunami Warning System Project Proposal, edited, UNESCO Intergovernmental Oceanographic Commission.

Jiang, L., and P. H. LeBlond (1992), The coupling of a submarine slide and the surface waves which it generates, *Journal of Geophysical Research*, *97*, 12,731–712,744.

Kanamori, H. (1972), Mechanism of Tsunami Earthquakes, *Physics of the earth and planetary interiors 6*, 346-359.

Kato, T., et al. (2001), A new tsunami monitoring system using RTK-GPS, paper presented at International Tsunami Symposium, Seattle, Washington.

Kowalik, Z., and P. M. Whitmore (1991), An investigation of two tsunamis recorded at Adak, Alaska, *Science of Tsunami Hazards*, *9*, 67-83.

Lander, J. F., et al. (2002), A Brief History of Tsunamis in the Caribbean Sea, *Science of Tsunami Hazards*, *20*, 57.

Lander, J. F., et al. (1999), Use of tsunami histories to define the local Caribbean hazard, paper presented at International Symposium on Marine Positioning, Melbourne, Florida, December.

Mader, C. L. (2001), Modeling the 1755 Lisbon tsunami generation and propagation across the Atlantic Ocean to the Caribbean, *Science of Tsunami Hazards*, *19*, 93-98.

Martin, P. J. (2000), A description of the Navy Coastal Ocean Model Version 1.0, 39 pp, Naval Research Laboratory, Stennis Space Center, MS.

McCann, W. R. (2006), Estimating the threat of tsunamigenic earthquakes and earthquake induced-landslide tsunami in the Caribbean, paper presented at NSF Caribbean Tsunami Workshop, World Scientific, San Juan, Puerto Rico.

Mercado, A., and W. McCann (1998), Numerical simulation of the 1918 Puerto Rico tsunami, *Natural Hazards*, *18*, 57-76.

Meyer, H., and J. H. Caicedo O. (1998), Evaluation of tsunami worse scenarios in the Caribbean Sea and simulation of wave weights – a TIME project activity (Oral Poster), paper presented at Okushiri Tsunami/UJNR Workshop.

Morey, S. L., et al. (2003b), Export pathways for river discharged fresh water in the northern Gulf of Mexico, *Journal of Geophysical Research*, *108*, 3303-3318.

Morey, S. L., et al. (2003a), The annual cycle of riverine influence in the eastern Gulf of Mexico basin, *Geophysical Research Letters*, *30*, 1867-1871.

Murty, T. S. (1977), Seismic Sea Waves: Tsunamis, *Bulletin of the Fisheries Research Board of Canada*, *Bull. 198*.

NGDC (2001), 2-Minute Gridded Global Relief Data (ETOPO2), edited, National Geophysical Data Center, NOAA Satellite and Information Service.

NGDC Tsunami Database (2005), edited, National Geophysical Data Center, NOAA Satellite and Information Service.

NOAA and USGS Fact Sheet (2005), Tsunami Detection and Warnings, edited, United States Department of Commerce, United States Department of the Interior.

O'Loughlin, K. F., and J. F. Lander (Eds.) (2003), *Caribbean Tsunamis: A 500-Year History from 1498-1998*, 263 pp., Kluwer Academic Publishers, Dordrecht.

Okada, Y. (1985), Surface deformation due to shear and tensile faults in a half space, *Bulletin of the Seismological Society of America*, *75*, 1135-1154.

Okal, E. A., et al. (2003), The deficient T waves of tsunami earthquakes, *Geophysical Journal International*, *152*, 416-432.

Pararas-Carayannis, G. (2004), Volcanic tsunami generating source mechanisms in the eastern Caribbean region, *Science of Tsunami Hazards*, *22*, 74-114.

Polet, J., and H. Kanamori (2000), Shallow subduction zone earthquakes and their tsunamigenic potential, *Geophysical Journal International*, *142*, 684-702.

Reid, H. F., and S. Taber (1919), The Porto Rico earthquake of 1918, House of Representatives, 66th Congress, 1st Session, Washington D.C., United States.

Rueda, F. J., and S. G. Schladow (2002), Quantitative comparison of models for barotropic response of homogeneous basins, *Journal of Hydraulic Engineering*, *128*, 201.

Shuto, N. (1991), Numerical simulations of tsunamis – its present and near future, *Natural Hazards*, *4*, 171-191.

Sigurdsson, H. R. (1996), Volcanic Tsunamis, Summary Report for the UNESCO IOC IOCARIBE Tsunami Warning Workshop, UNESCO IOC IOCARIBE, Paris.

Smith, M. S., and J. B. Shepherd (1994), Explosive submarine eruptions of Kick'em Jenny volcano: Preliminary investigations of the potential tsunami hazard in the eastern Caribbean region, paper presented at Caribbean Conference on Natural Hazards; volcanoes, earthquakes, windstorms, floods, St. Ann's Trinidad and Tobago, October 11-15.

Smith, M. S., and J. B. Shepherd (1995), Potential Cauchy-Poisson waves generated by submarine eruptions of Kick 'em Jenny volcano, *Natural Hazards*, *11*, 75-94.

Sykes, L. R., et al. (1982), Motion of Caribbean plate during the last 7 million years and implications for earlier cenozonic movements, *Journal of Geophysical Research*, *70*, 5065-5074.

ten Brink, U. S., et al. (2004), New seafloor map of the Puerto Rico Trench helps assess earthquake and tsunami hazards, *EOS, Transactions, American Geophysical Union*, *85*, 349-360.

Titov, V. V., et al. (2001), Project SIFT (Short-term Inundation Forecasting for Tsunamis), paper presented at International Tsunami Symposium, Seattle, Washington.

Todorovska, M. I., and M. D. Trifunac (2001), Generation of tsunamis by slowly spreading uplift of the sea floor, *Soil Dynamics and Earthquake Engineering*, *21*, 151-167.

von Hillebrandt-Andrade, C. (2006), Personal Correspondence, Puerto Rico Tsunami Ready Tide Gauge Network; Puerto Rico Seismic Network.

von Huene, R., et al. (1989), A large tsunamigenic landslide and debris flow along the Peru trench, *Journal of Geophysical Research*, *94*, 1703-1714.

Watts, P., et al. (2003), Landslide tsunami case studies using a Boussinesq model and a fully nonlinear tsunami generation model, *Natural Hazards and Earth System Sciences*, *3*, 391-402.

Weissert, T. P. (1990), Tsunami travel time charts for the Caribbean, *Science of Tsunami Hazards*, *8*, 67-78.

Whitmore, P. M. (2003), Tsunami amplitude prediction during events: A test based on previous tsunamis, *Science of Tsunami Hazards*, *21*, 135-143.

Woods Hole, Oceanographic Institution (2005), Major Caribbean earthquakes and tsunamis a real risk, edited, SCI/TECH. YubaNet.com.

Zahibo, N., et al. (2003b), Estimation of far-field tsunami potential for the Caribbean coast based on numerical simulation, *Science of Tsunami Hazards*, *21*, 202-222.

Zahibo, N., et al. (2003a), The 1867 Virgin Island tsunami: observations and modeling, *Oceanologica Acta*, *26*, 609-621.